

Article

Vanadium Pentoxide-Based Composite Synthesized Using Microwave Water Plasma for Cathode Material in Rechargeable Magnesium Batteries

Masashi Inamoto ^{1,2,*}, Hideki Kurihara ² and Tatsuhiko Yajima ¹

¹ Department of Applied Chemistry, Graduate School of Engineering, Saitama Institute of Technology, 1690, Fusaiji, Fukaya-shi, Saitama 369-0293, Japan; E-Mail: yajima@sit.ac.jp

² Saitama Industrial Technology Center, 3-12-18, Kamiaoki, Kawaguchi-shi, Saitama 333-0844, Japan; E-Mail: kuri@saitec.pref.saitama.jp

* Author to whom correspondence should be addressed; E-Mail: inamoto-m@saitec.pref.saitama.jp
Tel: +81-48-265-1420; Fax: +81-48-265-1334.

Received: 26 July 2013; in revised form: 6 September 2013 / Accepted: 6 October 2013 /

Published: 11 October 2013

Abstract: Multivalent cation rechargeable batteries are expected to perform well as high-capacity storage devices. Rechargeable magnesium batteries have an advantage in terms of resource utilization and safety. Here, we report on sulfur-doped vanadium pentoxide (S-V₂O₅) as a potential material for the cathodes of such a battery; S-V₂O₅ showed a specific capacity of 300 mAh g⁻¹. S-V₂O₅ was prepared by a method using a low-temperature plasma generated by carbon felt and a 2.45 GHz microwave generator. This study investigates the ability of S-V₂O₅ to achieve high capacity when added to metal oxide. The highest recorded capacity (420 mAh g⁻¹) was reached with MnO₂ added to composite SMn-V₂O₅, which has a higher proportion of included sulfur than found in S-V₂O₅. Results from transmission electron microscopy, energy-dispersive X-ray spectroscopy, Micro-Raman spectroscopy, and X-ray photoelectron spectroscopy show that the bulk of the SMn-V₂O₅ was the orthorhombic V₂O₅ structure; the surface was a xerogel-like V₂O₅ and a solid solution of MnO₂ and sulfur.

Keywords: microwave; rechargeable magnesium battery; cathode material; vanadium pentoxide; sulfur; manganese

1. Introduction

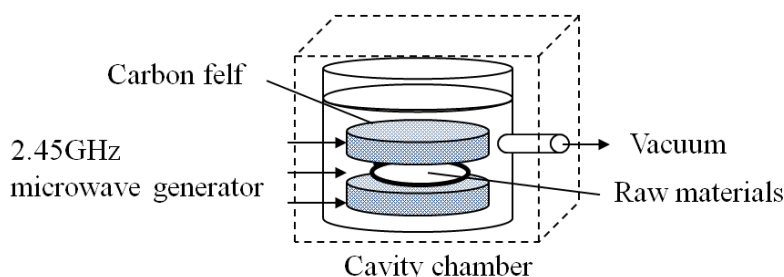
Recently, high-capacity rechargeable batteries have seen wide adoption as a power source for electric vehicles. Rechargeable magnesium batteries, which have been studied for a long time, have attracted attention for use in next-generation power storage applications. Aurbach *et al.* reported an electrolyte solution that allowed magnesium to dissolve and deposit reversibly [1,2].

However, there are a limited number of possible materials to use for the cathode of rechargeable magnesium batteries. In one case, Mg^{2+} is easily trapped in the cathode where it diffuses slowly. And, in another, repetitive insertion/desorption of Mg^{2+} at the cathode by use of high voltage can induce structural failure of the cathode or its dissolution into the electrolyte solution. Thus, one drawback of rechargeable magnesium batteries is the difficulty of maintaining their cycle characteristics because of their capacity fading [3,4].

For all of these reasons, there is high demand for cathode materials capable of stable insertion/desorption of Mg^{2+} in order to create a feasible rechargeable magnesium battery. The most commonly studied cathode materials are metal oxides [5,6] and metal sulfides [7,8]. As a rule, metal oxides possess stable crystal architecture but easily trap Mg^{2+} . On the other hand, metal sulfides are less likely to trap Mg^{2+} because their structure is generally unsound. Since sulfides have generally rather lower bond-energy than oxides, those are thought to be unsuitable for the cathode material for lithium-ion batteries. Our research is advancing toward a solution to the above problem. A summary of our results is given below.

Sulfur-doped vanadium pentoxide (S- V_2O_5) prepared by the method described in Section 3.1 was tested as an adaptation for the cathode of a rechargeable magnesium battery [9]. Our method employs low-temperature plasma generated using carbon felt and a 2.45 GHz microwave generator (CF-MWP, Figure 1) [10]. Structural analysis and charge-discharge characteristic evaluation were performed for S- V_2O_5 prepared by CF-MWP.

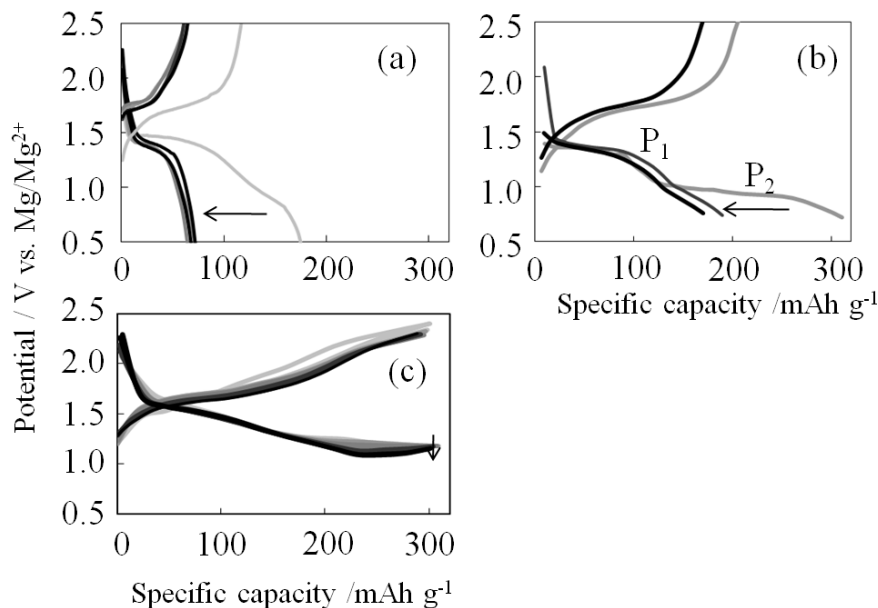
Figure 1. Schematic diagram of carbon felt and a 2.45 GHz microwave generator (CF-MWP).



Charge-discharge capacity curves are shown in Figure 2. For the orthorhombic V_2O_5 (Figure 2a), the first-cycle discharge was 170 mAh g^{-1} , and the second-cycle discharge was 70 mAh g^{-1} . This result is similar to that reported by Yu *et al.* [11]. For the composite of V_2O_5 and sulfur (Figure 2b) formed by simple mixing, two plateau potentials (P_1 and P_2) appeared at 1.4 V and 1.0 V *versus* Mg/Mg^{2+} due to V_2O_5 and sulfur, respectively. P_2 appeared in the first discharge cycle but did not appear after the second discharge cycle. One possible reason is that the sulfur may have been transferred to the electrolyte solution at the first Mg^{2+} desorption. However, the discharge capacity curve of S- V_2O_5

(Figure 2c) was 300 mAh g^{-1} and decreased in a linear fashion from 1.6 V to 1.0 V *versus* Mg/Mg^{2+} . This result implies that the surface of S- V_2O_5 became amorphous [12].

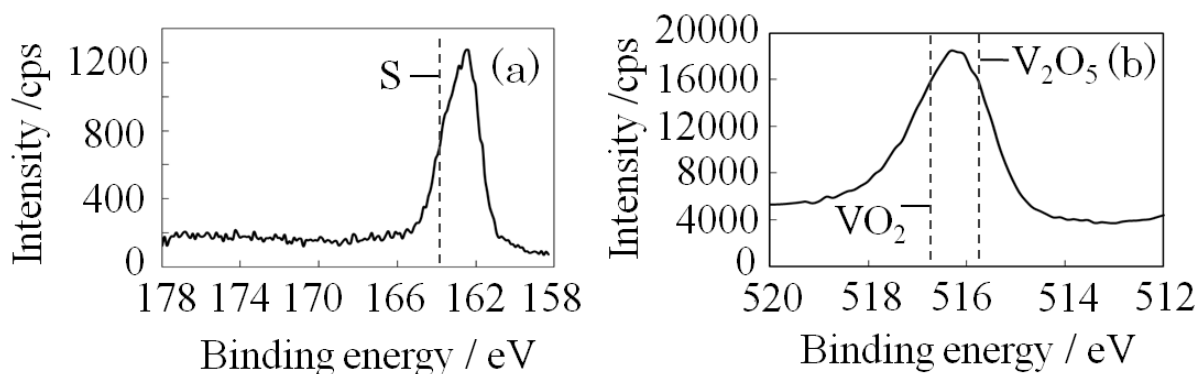
Figure 2. Charge-discharge curves: (a) V_2O_5 ; (b) Mixture of S and V_2O_5 ; and (c) S- V_2O_5 .



The X-ray photoelectron spectroscopy (XPS) results for S- V_2O_5 (Figure 3) showed that the S2p spectrum shift occurred at low energy and the $\text{V}2\text{p}_{3/2}$ spectrum shift occurred at a high energy. These results indicate a V-S bond-like state at the surface of S- V_2O_5 because of the solid solution formation of sulfur and V_2O_5 . Results of FTIR, XRD, SEM, and EPMA testing indicate that the surface of S- V_2O_5 was amorphous, similar to a xerogel structure, and that the bulk was the orthorhombic V_2O_5 .

The electrolyte after a charge-discharge cycle of S- V_2O_5 electrode included sulfur, which it did not include originally. This suggests that sulfur leached from the S- V_2O_5 electrode into the electrolyte through Mg^{2+} intercalation and desorption. Therefore, this study discusses the addition of a metal oxide material to inhibit sulfur elution.

Figure 3. X-ray photoelectron spectroscopy (XPS) narrow spectra of S- V_2O_5 : (a) S2p; and (b) $\text{V}2\text{p}_{3/2}$.

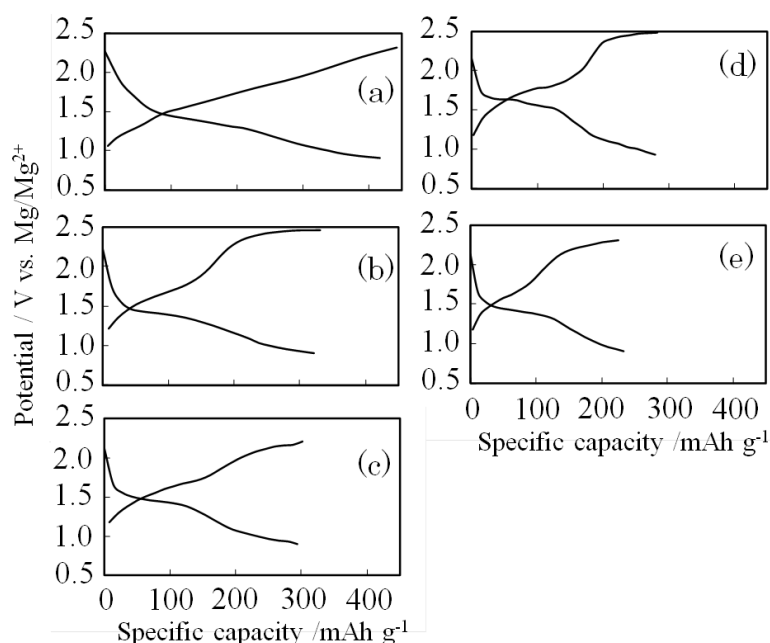


2. Results and Discussion

2.1. Electrochemical Characteristics

Charge-discharge capacity curves are shown in Figure 4. The discharge capacities of the batteries containing metal oxides (MnO_2 , MoO_3 , Fe_2O_3 , NiO , and ZrO_2) as additives were 420 mAh g^{-1} , 320 mAh g^{-1} , 300 mAh g^{-1} , 290 mAh g^{-1} , and 230 mAh g^{-1} , respectively. The highest capacity was reached in the case of MnO_2 ($\text{SMn-V}_2\text{O}_5$). The discharge curve in the case of $\text{SMn-V}_2\text{O}_5$ decreased linearly from 1.5 V to 0.9 V *versus* Mg/Mg^{2+} . This result demonstrates that the surface of the $\text{SMn-V}_2\text{O}_5$ was amorphous, similar to a xerogel structure; in this regard, it is similar to $\text{S-V}_2\text{O}_5$. Although the discharge curve obtained with added MoO_3 decreased linearly from 1.5 V to 0.9 V *versus* Mg/Mg^{2+} , its charge curve showed plateau potentials at around 1.8 V and 2.4 V. In the other curves, a plateau potential appeared at 1.5 V, and each of the curves descended abruptly after the plateau potential. The cathode formed by the addition of NiO had the highest plateau potential at 1.65 V, different from other cases. This result shows that the addition of NiO might improve the high-voltage characteristics of the obtained material. The metal oxides other than MnO_2 inhibited the formation of an $\text{S-V}_2\text{O}_5$ amorphous structure and showed a plateau potential.

Figure 4. Charge-discharge curves at second cycle: (a) MnO_2 ; (b) MoO_3 ; (c) Fe_2O_3 ; (d) NiO ; and (e) ZrO_2 .



2.2. Structural Analysis

A transmission electron microscopy (TEM) image, electron beam diffraction image, and energy dispersive X-ray spectrometry (EDX) spectrum of $\text{SMn-V}_2\text{O}_5$ are shown in Figures 5 and 6. The bulk of the $\text{SMn-V}_2\text{O}_5$ produced a clear image of electron diffraction. This result corresponds with the pattern of the orthorhombic V_2O_5 . Therefore, the bulk of the $\text{SMn-V}_2\text{O}_5$ has maintained the V_2O_5 the orthorhombic structure without degradation. In the TEM image, the surface of $\text{SMn-V}_2\text{O}_5$ is seen as a

thin layer with two types of morphology, shown in Figure 5 as Points 1 and 2. The diffraction image of Point 1 has a clear diffraction pattern and halo pattern. This diffraction pattern is slightly broader than the pattern for the orthorhombic V_2O_5 , and the observation of the halo pattern indicates an amorphous structure. The EDX spectrum at Point 1 shows a strong V peak. These results indicate that Point 1 was a V_2O_5 xerogel or a similar structure. This is similar to the case of S- V_2O_5 . The diffraction image of Point 2 shows only a halo pattern, and the EDX spectrum shows peaks for manganese and sulfur. Because these results indicate that Point 2 has an amorphous structure and consists of only manganese and sulfur, it is likely that Point 2 is a solid solution of MnO_2 and sulfur.

Figure 5. Transmission electron microscopy (TEM) of S-Mn- V_2O_5 and electron beam diffraction at Points 1 and 2.

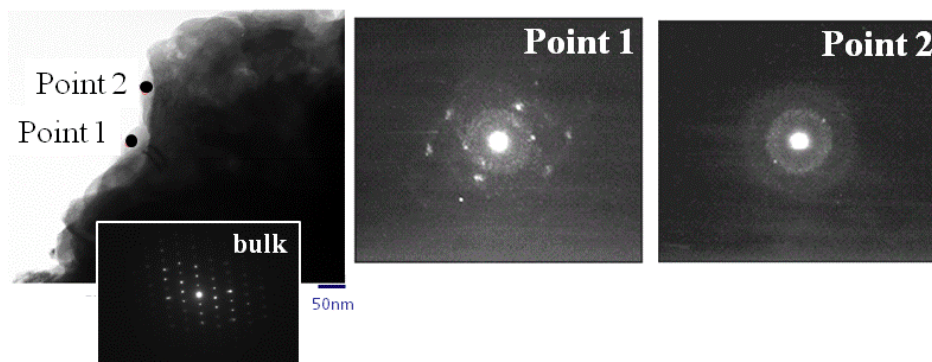
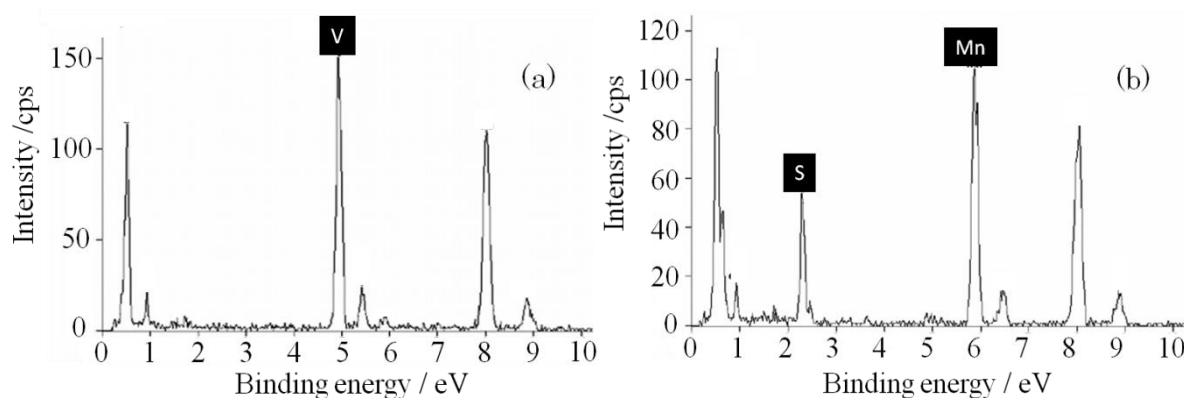


Figure 6. Energy dispersive X-ray spectrometry (EDX) at (a) Point 1; and (b) Point 2.

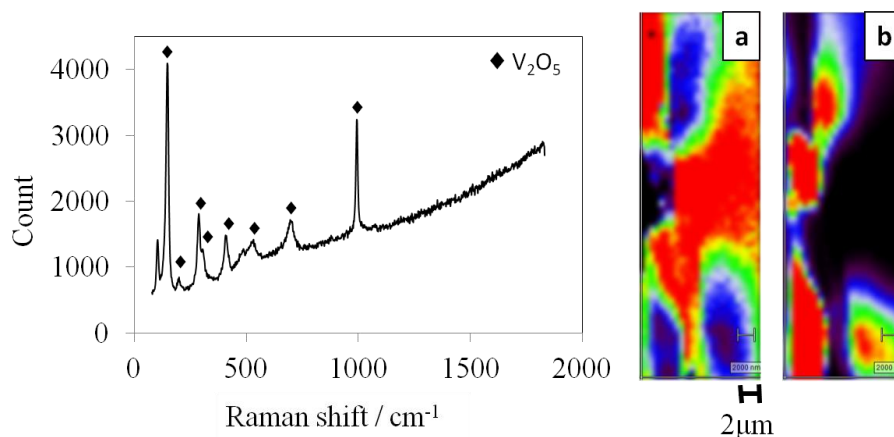


The micro-Raman spectrum of an SMn- V_2O_5 electrode is shown in Figure 7. The orthorhombic V_2O_5 peaks [13] and fluorescence can be seen, whereas there are no MnO_2 and sulfur peaks. This result indicates fluorescence, possibly derived from MnO_2 and sulfur. Thus, during Raman spectroscopy, although the area of fluorescence was low in intensity for V_2O_5 , the orthorhombic V_2O_5 and the fluorescence area were separate. These results, together with the results from TEM and EDX tests, suggest that the fluorescence area was a solid solution of MnO_2 and sulfur, indicating that SMn- V_2O_5 had a surface of the orthorhombic V_2O_5 covered with a solid solution. This is consistent with the TEM and EDX data.

The XPS narrow spectrum of SMn- V_2O_5 is shown in Figure 8. The peaks for $V2p_{3/2}$ and $S2p$ at the same positions as S- V_2O_5 suggest a S-V bond-like state and indicate an amorphous structure. The FWHM of SMn- V_2O_5 increased 2-fold compared to S- V_2O_5 . Therefore, there was considered that the

oxidation state of V of SMn-V₂O₅ have slightly different compared to S-V₂O₅. Mn2p_{3/2} became a solid-solution formation with sulfur, according to another analysis. The ratio of manganese to sulfur was about 1:2. This ratio remained constant when the amount of sulfur was increased five-fold. These results demonstrate that MnO₂ and sulfur were linked by mechanical force rather than by a chemical binding force. The ICP-MS analysis result shows that the molar ratio of V:Mn:S was 100:6.8:14.4. The sulfur content of SMn-V₂O₅ was twice that of S-V₂O₅ (V:S = 100:7.8). The ratio of manganese to sulfur was about 1:2 in SMn-V₂O₅; this result was arrived at by XPS analysis.

Figure 7. Raman spectroscopy of SMn-V₂O₅ and Raman images of the surface of the SMn-V₂O₅ of (a) V₂O₅; and (b) the fluorescence area.



Balanced chemical reactions involving V₂O₅, MnO₂, and S, along with their theoretical capacities, are shown below.

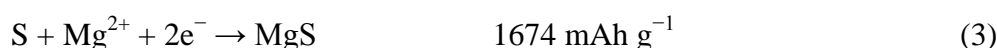
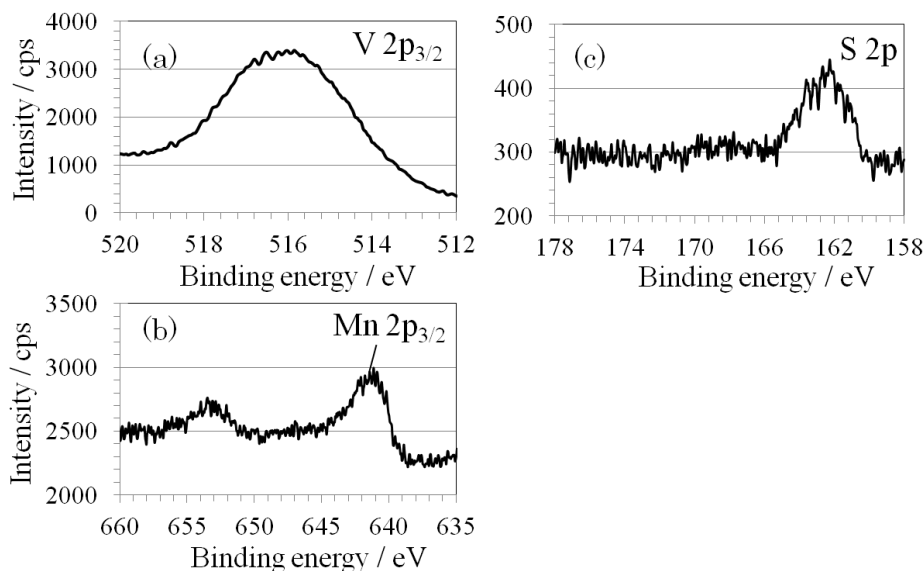


Figure 8. XPS narrow spectra of SMn-V₂O₅: (a) V2p_{3/2}; (b) Mn2p_{3/2}; and (c) S2p.



From the results of ICP-MS analysis and the three equations above, average theoretical capacities of SMn-V₂O₅ and S-V₂O₅ through the surface to bulk are calculated to be 458 mAh g⁻¹ and 393 mAh g⁻¹, respectively. That is, the empirically obtained capacity of SMn-V₂O₅ was 91.7% of the theoretical capacity. Because the theoretical capacity of MnO₂ is as high as that of V₂O₅, achieving a high capacity for SMn-V₂O₅ may be possible by increasing the amount of sulfur.

3. Experimental Section

3.1. Preparation of Cathode Material by CF-MWP

Vanadium pentoxide (V₂O₅), sulfur, and a metal oxide (MnO₂, MoO₃, Fe₂O₃, NiO, or ZrO₂) were mixed at a molar ratio of 2:1:1 in a ball mill (P-6, Fritsch Co., Ltd.). Additionally, the composite added MnO₂ was prepared the composite the ratio of 2:5:1 because of observing increase of sulfur contained amount. This composite was wetted down and left overnight, after which it was treated by our method involving low-temperature plasma generated using carbon felt and a 2.45 GHz microwave generator (CF-MWP). Specifically, 2.0 g of each raw material were placed between pieces of carbon felt (30 mm in diameter) and a 500 W, 2.45 GHz microwave was used to irradiate the material under reduced pressure (0.001 MPa) for 2 min (Figure 1) to synthesize the hybrid cathode materials. In this process, raw materials are treated by plasma formed from water in the raw materials as a result of electric discharge between the pieces of carbon felt. It is assumed that the water in the raw materials is distributed uniformly enough that the composite is treated uniformly. Furthermore, although the process was performed under reduced pressure and at the evaporating temperature of water, the process did not induce reduction of V₂O₅ and oxidation of sulfur.

3.2. Electrochemical Characteristics

The electrodes were prepared from a mixture of the cathode material, acetylene black, and a polyvinylidene fluoride binder with *N*-methyl-2-pyrrolidone with a weight ratio of 10:3:1. The resulting slurry was spread on carbon paper. The electrode was dried at 110 °C for 1.5 h. S-V₂O₅ was charged with magnesium ions and used as a counter electrode. This electrode showed the same potential changes as a magnesium alloy plate. A magnesium alloy plate was used as the reference electrode. For the electrolytic solution, 0.3 M Mg(ClO₄)₂ and 1.8 M H₂O dissolved in propylene carbonate were used, and the electrode performance was evaluated using three-electrode cells. The electrolyte has been proven for metal oxides as cathode active materials to charge and discharge smoothly [4]. The stability of the Mg pseudo reference electrode used was preliminarily checked to be stable by observing the reproducibility of cyclic voltammograms of ferrocene using the electrolytic solution containing 0.2 M ferrocene, 0.3 M Mg(ClO₄)₂ and 1.8 M H₂O in propylene carbonate solvent and an electrochemical system with a magnesium alloy plate as the reference electrode and platinum wires as working and counter electrodes. Charge-discharge tests were conducted between cut-off potentials from 2.4 V to 0.9 V *versus* Mg/Mg²⁺ at a constant current of 60 mA g⁻¹ (0.1 C). All trials were conducted at 25 °C.

3.3. Structural Analysis

The as-prepared samples were characterized by TEM (HF2000, Hitachi, Japan), EDX (Noran System SIX, Thermo Fisher Scientific, USA), micro-Raman spectroscopy (in Via Reflex/StreamLine, Renishaw, UK), and XPS (Quantum 2000, PHI, Inc.). The Raman spectroscopy measurements were taken after the electrodes were prepared.

4. Conclusions

As a cathode material for rechargeable magnesium batteries, we synthesized S-V₂O₅ with an added metal oxide prepared by CF-MWP and examined its crystal structure and electrode characteristics. The composite of V₂O₅, sulfur, and MnO₂ (SMn-V₂O₅) synthesized by CF-MWP demonstrated the highest capacity of 420 mAh g⁻¹ of any of the prepared samples. The charge-discharge curves showed that the SMn-V₂O₅ capacity decreased linearly from 1.5 V to 0.9 V but that, for the other electrodes, a plateau potential appeared at 1.5 V. This result was interpreted to mean that only SMn-V₂O₅ had a surface structure resembling a xerogel. The composite of V₂O₅, sulfur, and MnO₂ was treated by CF-MWP. The bulk of the resulting composite was orthorhombic V₂O₅, while the surface showed a xerogel-like structure of V₂O₅ and a solid solution of sulfur and MnO₂.

Acknowledgments

The authors thank Shimadzu Techno-Research, Inc. for providing equipment used in Raman spectroscopic measurements. We are grateful to Shimadzu Techno-Research.

Conflicts of Interest

The authors declare no conflict of interest.

References

1. Aurbach, D.; Lu, Z.; Schechter, A.; Gofer, Y.; Gizbar, H.; Turgeman, R.; Cohen, Y.; Moshkovich, M.; Levi, E. Prototype systems for rechargeable magnesium batteries. *Nature* **2000**, *407*, 724–727.
2. Aurbach, D.; Cohen, Y.; Moshkovich, M. The study of reversible magnesium deposition by *in situ* scanning tunneling microscopy. *Electrochem. Solid State Lett.* **2001**, *4*, A113–A116.
3. Novák, P.; Scheifele, W.; Haas, O. Magnesium insertion batteries—An alternative to lithium? *J. Power Sources* **1995**, *54*, 479–482.
4. Novák, P.; Scheifele, W.; Joho, F.; Haas, O. Electrochemical insertion of magnesium into hydrated vanadium bronzes. *J. Electrochem. Soc.* **1995**, *142*, 2544–2550.
5. Novák, P.; Desilvestro, J. Electrochemical insertion of magnesium in metal oxides and sulfides from aprotic electrolytes. *J. Electrochem. Soc.* **1993**, *140*, 140–144.
6. Feng, Z.; Yang, J.; NuLi, Y.; Wang, J. Sol-gel synthesis of Mg_{1.03}Mn_{0.97}SiO₄ and its electrochemical intercalation behavior. *J. Power Sources* **2008**, *184*, 604–609.
7. Tao, Z.L.; Xu, L.N.; Gou, X.L.; Chen, J.; Yuan, H.T. TiS₂ nanotubes as the cathode materials of Mg-ion batteries. *Chem. Commun.* **2004**, *18*, 2080–2081.

8. Mitelman, A.; Levi, M.D.; Lancry, E.; Levi, E.; Aurbach, D. New cathode materials for rechargeable Mg batteries: Fast Mg ion transport and reversible copper extrusion in CuMo_6S_8 compounds. *Chem. Commun.* **2007**, *41*, 4212–4214.
9. Inamoto, M.; Kurihara, H.; Yajima, T. Electrode performance of S-doped vanadium pentoxide as cathode active material for rechargeable magnesium battery. *Hyomen Gijutsu* **2011**, *62*, 516–520.
10. Kurihara, H.; Yajima, T. Decomposition of toluene by atmospheric pressure microwave plasma generated using metal salt-impregnated carbon felt pieces. *Chem. Lett.* **2007**, *36*, 526–527.
11. Yu, L.; Zhang, X. Electrochemical insertion of magnesium ions into V_2O_5 from aprotic electrolytes with varied water content. *J. Colloid Interface Sci.* **2004**, *278*, 160–165.
12. Imamura, D.; Miyayama, M. Characterization of magnesium-intercalated V_2O_5 /carbon composites. *Solid State Ion.* **2003**, *161*, 173–180.
13. Baddour-Hadjean, R.; Smirnov, M.B.; Smirnov, K.S.; Kazimirov, V.Y.; Gallardo-Amores, J.M.; Amador, U.; Arroyo-de Dompablo, M.E.; Pereira-Ramos, J.P. Lattice dynamics of β - V_2O_5 : Raman spectroscopic insight into the atomistic structure of a high-pressure vanadium pentoxide polymorph. *Inorg. Chem.* **2012**, *51*, 3194–3201.

© 2013 by the authors; licensee MDPI, Basel, Switzerland. This article is an open access article distributed under the terms and conditions of the Creative Commons Attribution license (<http://creativecommons.org/licenses/by/3.0/>).